

Molecular Interactions of Flavonoids to Hyaluronidase: Insights from Spectroscopic and Molecular Modeling Studies

Hua-jin Zeng¹ · Jiao Ma¹ · Ran Yang² · You Jing¹ · Ling-bo Qu^{2,3}

Received: 12 March 2015 / Accepted: 23 April 2015 / Published online: 26 May 2015
© Springer Science+Business Media New York 2015

Abstract In the work described on this paper, the interactions between eight flavonoids and hyaluronidase (HAase), an important enzyme involved in a promoting inflammation pathway, were investigated by spectroscopic and molecular modeling methods. The results revealed that all flavonoids could interact with HAase to form flavonoid-HAase complexes. The binding parameters obtained from the data at different temperatures indicated that flavonoids could spontaneously bind with HAase mainly through electrostatic forces and hydrophobic interactions with one binding site. According to synchronous and three-dimensional fluorescence spectra and the molecular docking results, all flavonoids bound directly into the enzyme cavity site and the binding of flavonoid into the enzyme cavity influenced the microenvironment of the HAase activity site which led to the reduced enzyme activity. The present study provides direct evidence at a molecular level to understand the mechanism of inhibitory effect of flavonoid against HAase and explain the anti-inflammatory mechanism of the Traditional Chinese Medicines as anti-inflammatory drugs.

Keywords Flavonoids · Hyaluronidase · Fluorescence spectroscopy · Molecular docking · Anti-inflammatory mechanism

✉ Ran Yang
yangran@zzu.edu.cn

¹ School of Pharmaceutical Sciences, Zhengzhou University, Zhengzhou 450001, People's Republic of China

² College of Chemistry and Molecular Engineering, Zhengzhou University, Zhengzhou 450001, People's Republic of China

³ School of Chemistry and Chemical Engineering, Henan University of Technology, Zhengzhou 450001, People's Republic of China

Introduction

Initially, the inflammation is a normal response to infection and tissue injury, but without an appropriate and timely treatment it can lead to the development of chronic diseases in human bodies [1, 2]. It was reported that there were several enzymes known to be involved in a promoting inflammatory pathway [3–5]. One of the most important enzymes in this process was hyaluronidase (HAase), which is a hyaluronic acid-splitting enzyme and is involved in the permeability of the vascular system and may directly control the mast cell degranulation [6]. Therefore, it can be deduced that the anti-inflammatory agents had a strong inhibitory effect on the activity of HAase. This result seemed to indicate that the potent HAase inhibitory substances might have anti-inflammatory effects, and could become leading compounds in the development of new anti-inflammatory drugs. On the basis of this information, in recent years many researchers have devoted to searching and detecting the inhibitory effects of some natural products against HAase [7–10].

Flavonoids, a group of important polyphenols that are widely present in foods of plant origin, have been proved to exhibit broad pharmaceutical activities [11, 12]. In recent years, many flavonoids, such as apigenin [13, 14], luteolin [15, 16], keampferol [17], quercetin [18], morin [19, 20], naringenin [21, 22], daidzein [23] and genistein [24, 25], have also been shown to possess anti-inflammatory and anti-allergic activities. These results suggested that flavonoids might have potential ability to inhibit the activity of HAase. And this view has been supported by previous studies [10, 26–28], which have proved that some flavonoids, including apigenin, luteolin, keampferol, quercetin and naringenin, had the inhibitory effect on HAase. However,

Fig. 1 The molecular structures of flavonoids

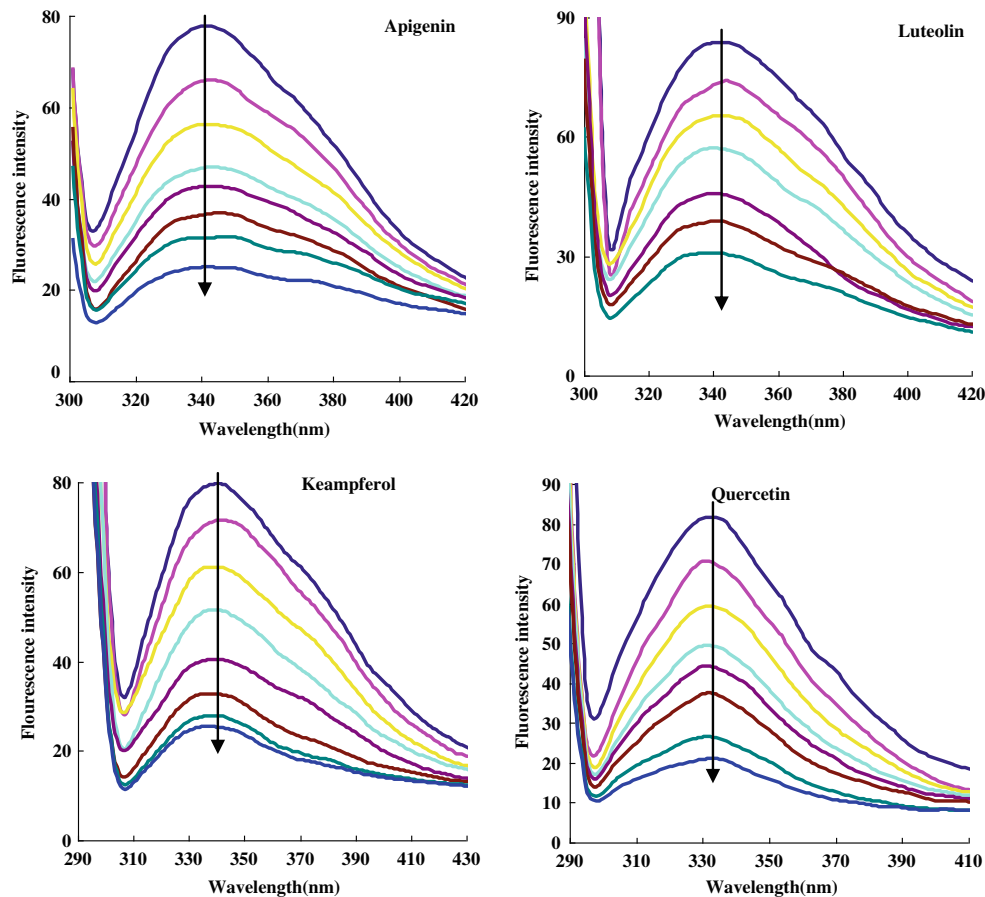
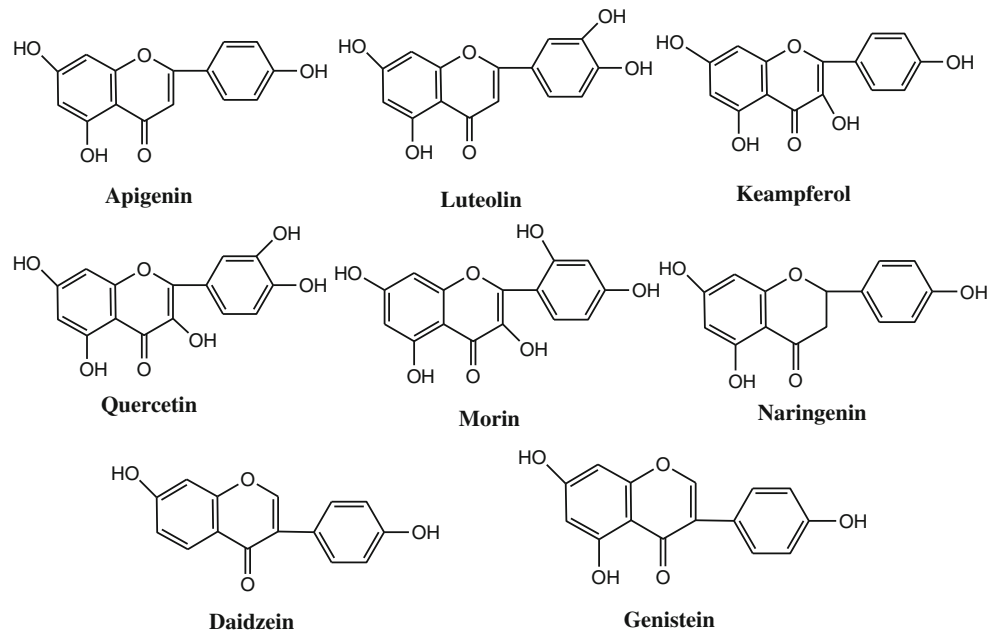


Fig. 2 Effect of flavonoids on HAase fluorescence. Conditions: peak from up to down $C_{\text{Apigenin}}=(0, 4, 8, 12, 16, 20, 24)\times 10^{-6} \text{ mol}\cdot\text{L}^{-1}$, $C_{\text{Luteolin}}=(0, 4, 10, 16, 24, 30, 36)\times 10^{-6} \text{ mol}\cdot\text{L}^{-1}$, $C_{\text{Keampferol}}=(0, 2, 4, 10, 16, 20, 24, 30)\times 10^{-6} \text{ mol}\cdot\text{L}^{-1}$; $C_{\text{Quercetin}}=(0, 4, 10, 16, 20, 24, 30,$

$36)\times 10^{-6} \text{ mol}\cdot\text{L}^{-1}$; $C_{\text{Morin}}=(0, 4, 10, 16, 24, 30, 36)\times 10^{-6} \text{ mol}\cdot\text{L}^{-1}$; $C_{\text{Naringenin}}=(0, 6, 12, 18, 24, 30, 36, 42)\times 10^{-6} \text{ mol}\cdot\text{L}^{-1}$; $C_{\text{Daidzein}}=(0, 10, 16, 20, 30, 40, 50)\times 10^{-6} \text{ mol}\cdot\text{L}^{-1}$; $C_{\text{Genistein}}=(0, 4, 8, 12, 16, 22, 24)\times 10^{-6} \text{ mol}\cdot\text{L}^{-1}$; $C_{\text{HAase}}=0.1\times 10^{-5} \text{ mol}\cdot\text{L}^{-1}$, $T=293 \text{ K}$

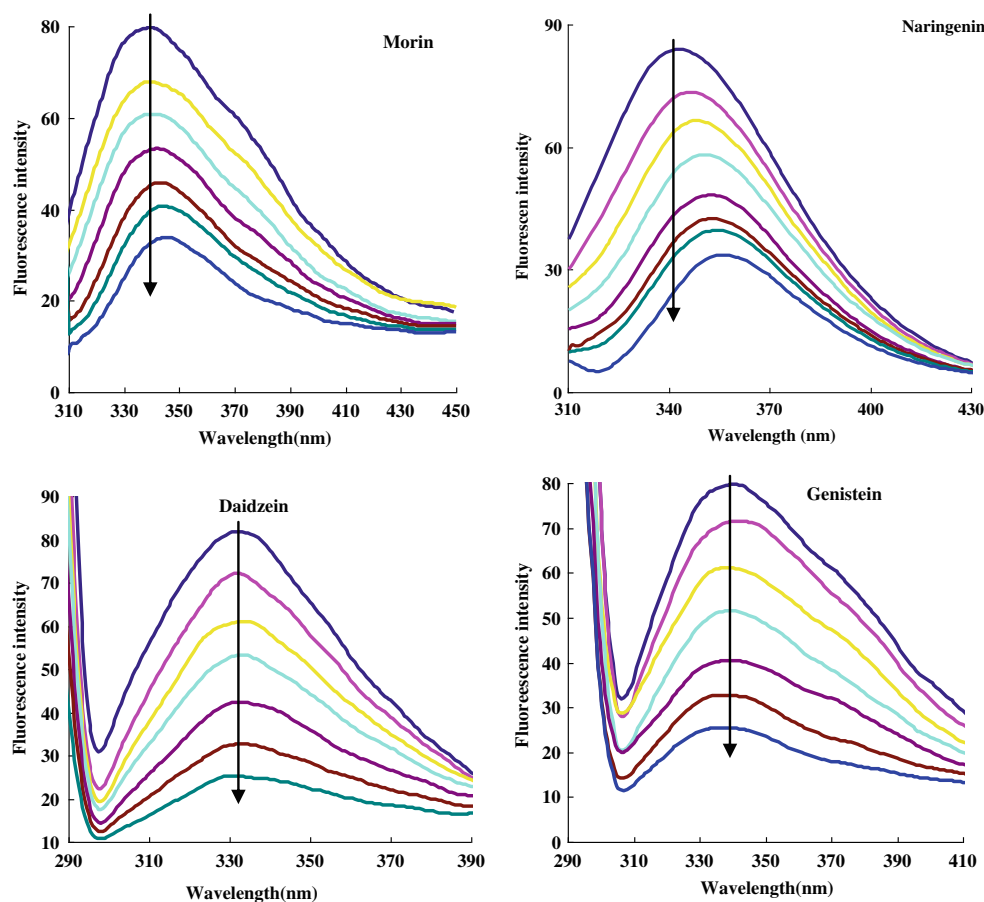


Fig. 2 continued.

these researches were limited to the enzymatic activity assay and the inhibitory mechanism of flavonoids on HAase has not been investigated. In addition, many herbal drugs, such as *Lysimachia christinae* Hance, *Tussilage farfara* L., *Ginkgo biloba* L., *Lonicera japonica* Thunb., *Sophora japonica* L., *Bupleurum chinense* DC., and *Pueraria lobata* (willd) Ohwi., have been widely used in clinic to treat various inflammations and allergies in China and have been officially listed in the China Pharmacopoeia as traditional Chinese medicines (TCMs) [29]. According to the China Pharmacopoeia, flavonoids are one of the major anti-inflammatory and anti-allergic ingredients of these herbal drugs. Therefore, it is very significant for clarifying the anti-inflammatory mechanism of TCMs to investigate on the binding of flavonoids with HAase.

In pharmacology, knowledge of the binding of inhibitors with protease can not only help to understand the metabolic process of inhibitors in body, but also help to reveal the inhibitory mechanism of protease inhibitors and accelerate the development of new inhibitors [30–32]. Thus, in the present study the bindings of 8 flavonoids (structures shown in Fig. 1) with HAase were investigated by spectroscopic

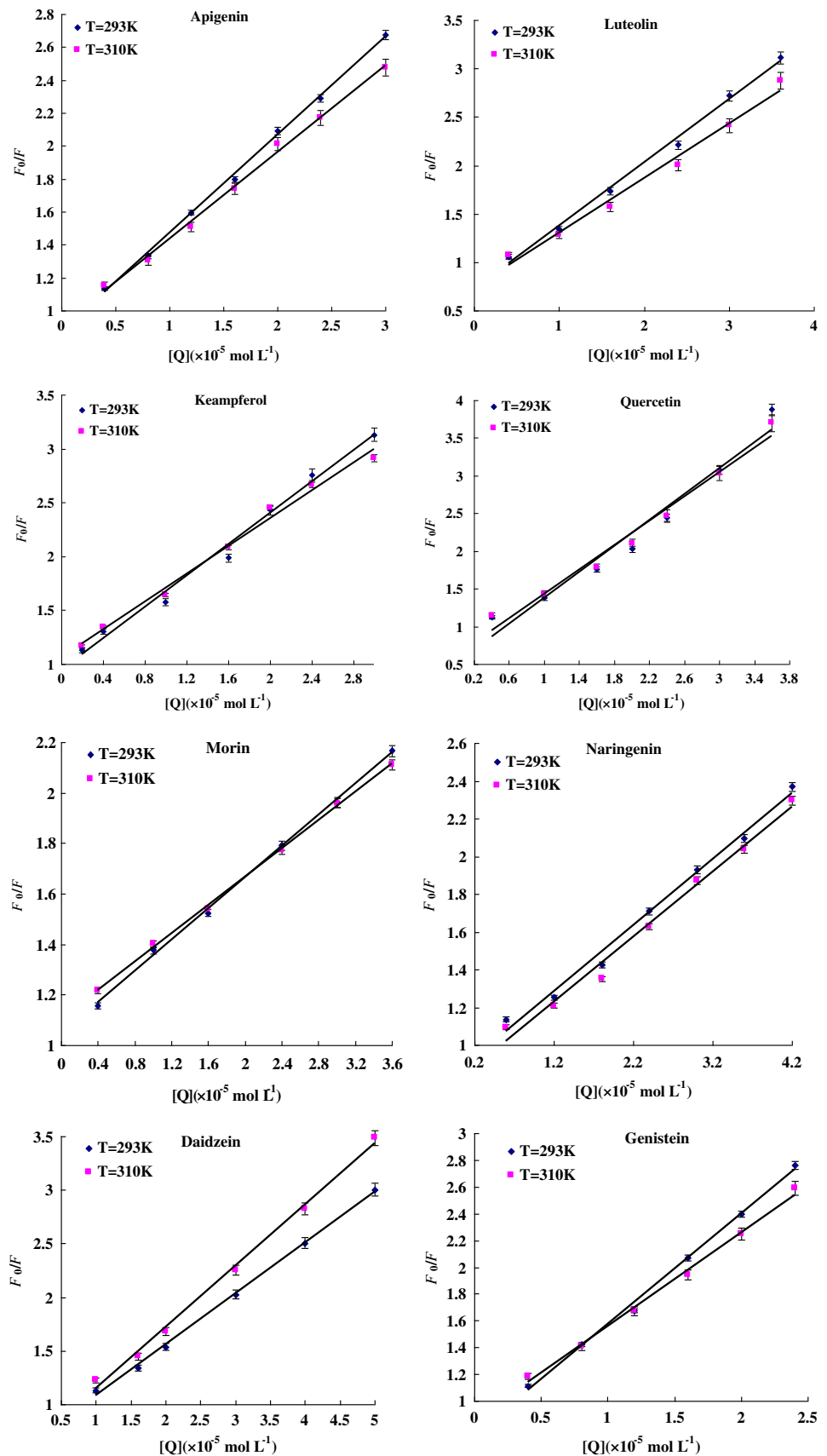
and molecular modeling methods. The binding parameters, including binding constant, thermodynamic parameters, binding distance and the number of binding site, and the effect of flavonoids on HAase conformation were evaluated. The aim of this work is to provide direct evidence at a molecular level to understand the inhibitory mechanism of flavonoids against HAase and explain the anti-inflammatory mechanism of the above TCMs as anti-inflammatory and anti-allergic drugs.

Experimental

Reagents

The HAase was purchased from Sigma-Aldrich Chemical Co. (USA) and was dissolved in ultra water to form a 1.0×10^{-5} mol L⁻¹ solution, then preserved at 4 °C. Flavonoids were obtained from the National Institute for the Control of Pharmaceutical and Biological Products (Beijing, China) and were dissolved in methanol to form a 1.0×10^{-3} mol L⁻¹ solution. A 0.2 mol L⁻¹ mixture of phosphate

Fig. 3 Stern-Volmer plots for the quenching of HAase by flavonoids at different temperature ($n=3$)



buffer was used to control the pH (pH=7.4). All the chemicals were of analytical-reagent grade and used without further purification. Water was purified with a Milli-Q purification system (Barnstead, USA).

Apparatus and Measurements

Fluorescence Measurements

All fluorescence spectra were recorded on a Hitachi F-2500 fluorescence spectrophotometer with a 1 cm quartz cell. The experimental temperature was maintained by recycling water throughout the quartz cell. The excitation wavelength was 280 nm and the excitation and emission slit widths were set at 10 nm. The scan speed was 1200 nm min⁻¹ and photo multiplier tube (PMT) voltage was 600 V.

Synchronous fluorescence spectra of HAase in the absence and presence of flavonoids were measured ($\Delta\lambda=15$ nm, $\lambda_{ex}=250-320$ nm and $\Delta\lambda=60$ nm, $\lambda_{ex}=250-320$ nm, respectively). The excitation and emission slit widths were set at 5 nm. The scan speed was 1200 nm min⁻¹ and PMT voltage was 600 V.

The three dimensional fluorescence spectra were performed under the following conditions: the emission wavelength range was selected from 270 to 500 nm, the initial excitation wavelength was set to 200 nm, and the scanning number was 15 with the increment of 10 nm.

Molecular Docking Investigation

Docking calculations were carried out using AutoDock 4.0. The structure of flavonoids was generated by Chemdraw Ultra 8.0 and the energy minimized conformation of flavonoids was obtained by Gaussian 03 software. Docking calculations were carried out on a HAase model (PDB code 2PE4, <http://www.rcsb.org/pdb/home/home.do>). With the aid of AutoDock, the ligand root of flavonoids was detected and rotatable bonds were defined. Essential hydrogen atoms and Kollman united atom type charges were added into the HAase protein model. Docking simulations were performed using the local search method to search for the optimum binding site of small molecules to the protein. To recognize the binding sites in HAase, blind docking was carried out and grid maps of 126 Å×126 Å×126 Å grid points and 0.375 Å spacing were generated. The AutoDocking parameters used were, GA population size: 100; maximum number of energy evaluations: 250,000. The conformation with the lowest binding free energy was used for further analysis.

Results and Discussion

Fluorescence Quenching

In the past few years, fluorescence has been widely applied to study the binding of drugs and proteins and can provide abun-

Table 1 Stern-Volmer constants for the interaction of hyaluronidase with flavonoids at different temperatures (n=3)

Flavonoid	T (K)	Equations	K_{sv} (L mol ⁻¹)	K_q (L mol ⁻¹)	R ^a	SD ^b
Apigenin	293	$F_0/F = 5.9640[Q] + 0.8740$	5.96×10^4	5.96×10^{12}	0.9991	0.09
	310	$F_0/F = 5.2605[Q] + 0.9106$	5.26×10^4	5.26×10^{12}	0.9979	0.11
Luteolin	293	$F_0/F = 6.5263[Q] + 0.7259$	6.53×10^4	6.53×10^{12}	0.9973	0.07
	310	$F_0/F = 5.6440[Q] + 0.7416$	5.64×10^4	5.64×10^{12}	0.9923	0.08
Keampferol	293	$F_0/F = 7.2644[Q] + 0.9458$	7.26×10^4	7.26×10^{12}	0.9947	0.13
	310	$F_0/F = 6.4506[Q] + 1.0628$	6.45×10^4	6.45×10^{12}	0.9955	0.15
Quercetin	293	$F_0/F = 8.5658[Q] + 0.5285$	8.57×10^4	8.57×10^{12}	0.9613	0.16
	310	$F_0/F = 8.0290[Q] + 0.6234$	8.03×10^4	8.03×10^{12}	0.9769	0.11
Morin	293	$F_0/F = 3.1002[Q] + 1.0437$	3.10×10^4	3.10×10^{12}	0.9984	0.12
	310	$F_0/F = 2.8055[Q] + 1.106$	2.81×10^4	2.81×10^{12}	0.9987	0.11
Naringenin	293	$F_0/F = 3.5028[Q] + 0.8625$	3.50×10^4	3.50×10^{12}	0.9952	0.10
	310	$F_0/F = 3.4442[Q] + 0.8156$	3.44×10^4	3.44×10^{12}	0.9937	0.11
Daidzein	293	$F_0/F = 5.7221[Q] + 0.5714$	5.72×10^4	5.72×10^{12}	0.9960	0.10
	310	$F_0/F = 4.7483[Q] + 0.6104$	4.75×10^4	4.75×10^{12}	0.9986	0.13
Genistein	293	$F_0/F = 8.2006[Q] + 0.7607$	8.20×10^4	8.20×10^{12}	0.9966	0.13
	310	$F_0/F = 7.0044[Q] + 0.8612$	7.00×10^4	7.00×10^{12}	0.9948	0.14

^a The correlation coefficient

^b The standard deviation

Fig. 4 Double-log plots of flavonoid quenching effect on HAase fluorescence at different temperature ($n=3$)

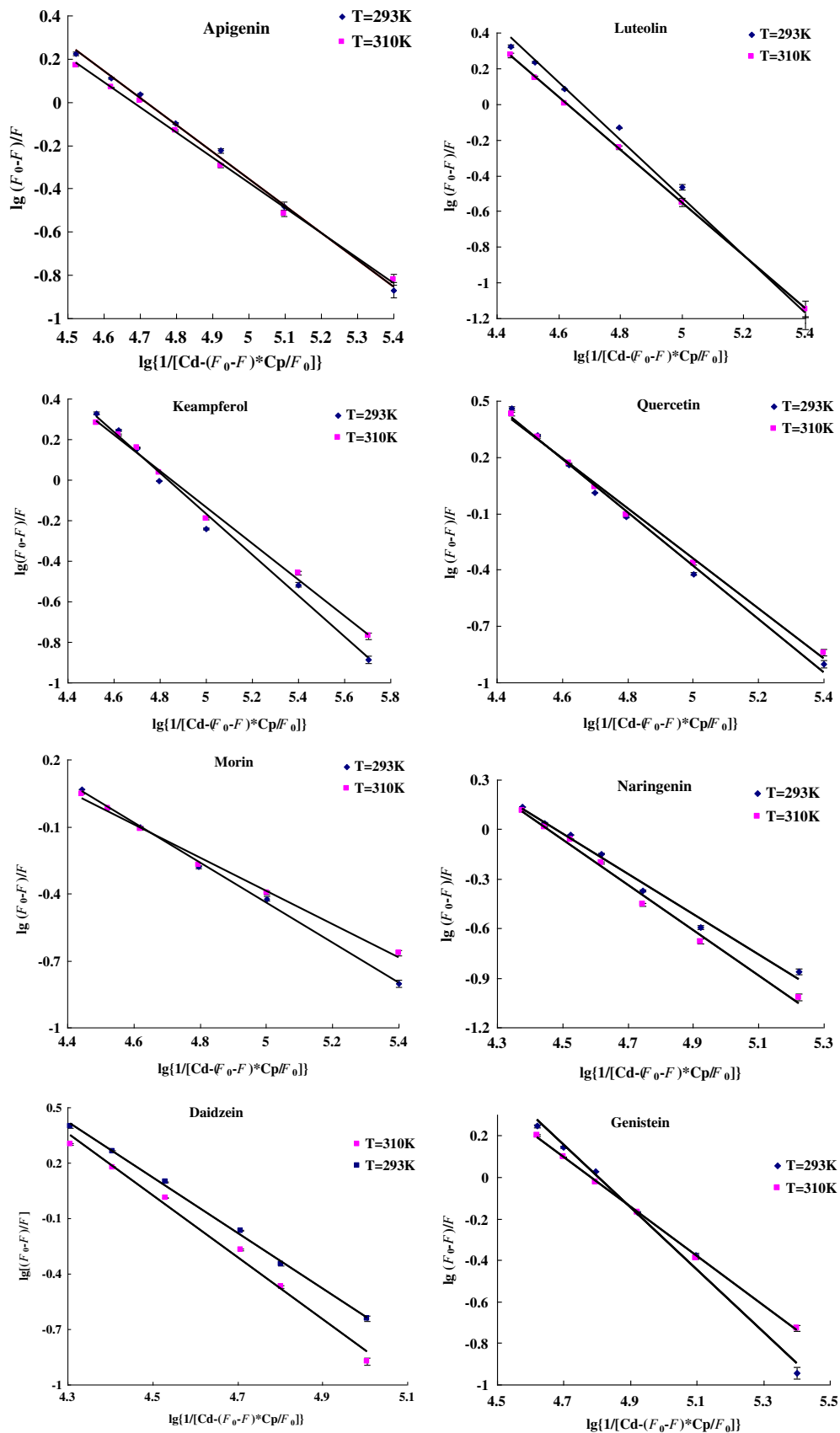


Table 2 The binding constant K_a and relative thermodynamic parameters of the flavonoid-hyaluronidase systems ($n=3$)

Flavonoid	T (K)	K_a (L mol ⁻¹)	n	R^a	SD ^b	ΔH° (kJ mol ⁻¹)	ΔG° (kJ mol ⁻¹)	ΔS° (J mol ⁻¹ K ⁻¹)
Apigenin	293	5.22×10^4	1.25	0.9989	0.04	-3.89	-26.46	77.02
	310	4.78×10^4	1.16	0.9985	0.06	-3.89	-27.77	77.02
Luteolin	293	5.90×10^4	1.61	0.9961	0.09	-2.17	-26.76	83.94
	310	5.62×10^4	1.45	0.9999	0.07	-2.17	-28.19	83.94
Keampferol	293	6.82×10^4	1.01	0.9951	0.07	-1.77	-27.11	86.49
	310	6.55×10^4	0.90	0.9970	0.05	-1.77	-28.58	86.49
Quercetin	293	5.42×10^4	1.42	0.9934	0.08	1.10	-26.55	94.36
	310	5.55×10^4	1.33	0.9961	0.05	1.10	-28.16	94.36
Morin	293	3.23×10^4	0.75	0.9939	0.05	-2.82	-25.28	76.70
	310	3.03×10^4	0.90	0.9982	0.04	-2.82	-26.34	76.70
Naringenin	293	3.01×10^4	1.22	0.9947	0.09	-2.24	-25.12	78.09
	310	2.86×10^4	1.37	0.9962	0.04	-2.24	-26.45	78.09
Daidzein	293	3.82×10^4	1.49	0.998	0.06	-6.88	-25.70	87.68
	310	3.27×10^4	1.68	0.9905	0.05	-6.88	-26.79	87.68
Genistein	293	6.37×10^4	1.50	0.9916	0.07	-2.44	-26.95	91.96
	310	6.03×10^4	1.19	0.9994	0.06	-2.44	-28.37	91.96

^a The correlation coefficient

^b The standard deviation

dant information about the binding parameters [33]. In this study, the technique was applied to investigate the interaction between flavonoids and HAase. The fluorescence spectra of HAase at different concentrations of flavonoids were shown in Fig. 2. As shown in Fig. 2, it could be seen that the fluorescence intensities of HAase decreased regularly with an increasing concentration of flavonoids, which indicated that flavonoids can bind to and alter the structure of HAase. Moreover, conspicuous changes of peak shape in the emission spectra of HAase were also found in morin-HAase system (red shift from 338 to 345 nm) and naringenin-HAase system (red shift from 338 to 355 nm), which suggested that the microenvironment of amino acid residues was changed after addition of these two flavonoids.

In order to distinguish static quenching from dynamic quenching by the temperature effects, fluorescence tests were performed at different temperatures. The quenching constant at each temperature was obtained by Stern-Volmer equation [34]:

$$F_0/F = 1 + K_{sv}[Q] = 1 + K_q\tau_0[Q] \quad (1)$$

where F_0 and F represent the fluorescence intensities in the absence and presence of flavonoids, respectively, and $[Q]$ is the concentration of the quencher (flavonoids here), K_{sv} is the Stern-Volmer quenching constant, which was determined by linear regression of Stern-Volmer equation. K_q , which equals K_{sv}/τ_0 , is the quenching rate constant of bio-molecular, while

τ_0 stands for the average fluorescence lifetime of the fluorophore in the absence of quencher and its value equals 10^{-8} s [35]. According to Eq. (1), the plots of Stern-Volmer at different temperatures were shown in Fig. 3 and the K_{sv} and K_q values were presented in Table 1.

Generally, the quenching constant decreases with the increasing temperature for static quenching, whereas the contrary effect is measured for dynamic quenching [36]. As shown in Table 1, the Stern-Volmer dynamic quenching constant K_{sv} decreased with the rising temperature, indicating that the probable quenching mechanism of fluorescence of HAase by flavonoids is not initiated by dynamic collision but complex formation. In other words, the fluorescence quenching of HAase resulted from complex formation is predominant; while from dynamic collision can be negligible. In general, the maximum scatter collision quenching constant K_q of various kinds of quenchers with biopolymer is 2.0×10^{10} L mol⁻¹ S⁻¹ [37]. However, the rate constants for the quenching of HAase caused by flavonoids are all greater than the K_q for the scatter mechanism. This confirms that the fluorescence quenching is not the result of dynamic collision quenching, rather a consequence of static quenching.

Binding Constant and the Number of Binding Sites

For the static quenching, when small molecules bind independently to a set of equivalent sites on a macromolecule, the equilibrium between free and bound molecules could be

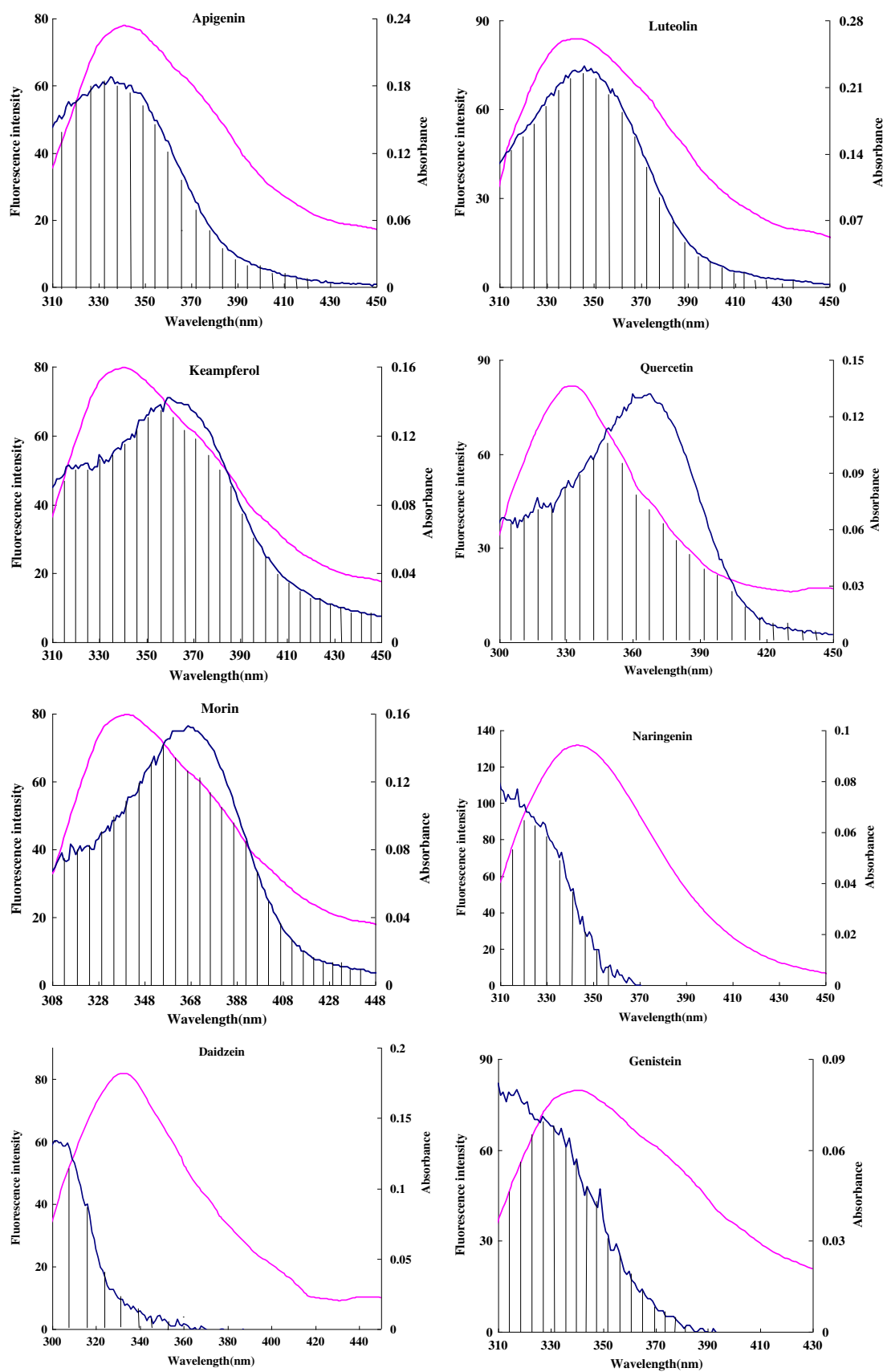


Fig. 5 Overlapping of fluorescence spectra of HAase ($C_{\text{HAase}}=0.1 \times 10^{-5} \text{ mol} \cdot \text{L}^{-1}$) with absorption spectra of flavonoids ($C_{\text{Flavonoid}}=0.1 \times 10^{-5} \text{ mol} \cdot \text{L}^{-1}$)

Table 3 The distance parameters of hyaluronidase with flavonoids

Flavonoid	J (cm ³ ·mol ⁻¹ ·L)	R_0 (nm)	E	r (nm)
Apigenin	1.54×10^{-14}	3.12	0.15	4.16
Luteolin	2.09×10^{-14}	3.29	0.06	5.26
Keampferol	3.12×10^{-14}	2.39	0.07	3.73
Quercetin	1.67×10^{-14}	3.17	0.08	4.71
Morin	1.62×10^{-14}	3.15	0.10	4.52
Naringenin	2.84×10^{-15}	2.36	0.12	3.28
Daidzein	8.68×10^{-15}	2.39	0.03	4.39
Genistein	3.95×10^{-15}	2.49	0.10	3.58

represented by the following equation [38]:

$$\log\left(\frac{F_0 - F}{F}\right) = n \log K_a - n \log\left\{\frac{1}{[C_d] - (F_0 - F)C_p} / F_0}\right\} \quad (2)$$

where K_a is static quenching constant, n is the number of binding sites per HAase molecule, $[C_d]$ and $[C_p]$ are the concentration of drug molecule (flavonoids) and protein (HAase), respectively. By plot of $\log(F_0 - F)/F$ versus $\log\{1/[[C_d] - (F_0 - F)C_p]/F_0\}$ (shown in Fig. 4), the number binding sites n and binding constant K_a of the interaction between HAase and flavonoids can be calculated and the results are summarized in Table 2. From Table 2, it can be seen that the numbers of binding sites n for flavonoids were all approximately to one at different temperatures, which suggested that one molecule of the protein combined with one molecule of flavonoids. The values of K_a for all flavonoids were of the order of 10^4 L mol⁻¹, indicating that a strong interaction exists between HAase and flavonoids. Moreover, by comparison of the binding constants of different flavonoids with HAase, it could be concluded that the amount and position of hydrogen-bond, double bond between C₂ and C₃ were the main structure characters that influenced their binding potencies which were consistent with the structure features that determine the inhibitory effects on HAase [26, 39]. This gives a clue that the determination of protein binding to structurally related compounds is a valuable tool for identifying the groups of a drug molecule.

The Force Acting Between HAase and Flavonoids

Thermodynamic parameters for an interaction can be used as a main evidence to understand the nature of intermolecular forces between drugs and protein [40]. According to thermodynamic equations:

$$\ln K = -\Delta H^\circ / RT + \Delta S^\circ / R \quad (3)$$

$$\Delta G^\circ = \Delta H^\circ - T \cdot \Delta S^\circ = -RT \ln K \quad (4)$$

where K is analogous to the effective quenching constants K_a at the same temperature and R is the gas constant. ΔS° , ΔH° and ΔG° show entropy change, enthalpy change and free energy change, respectively.

From the thermodynamic view point, ΔH° and ΔS° are positive, implying that the main interaction force is a hydrophobic interaction. However, ΔH and ΔS are negative, indicating that the main interaction force is Van der Waals forces or hydrogen bonding interaction. ΔH° is almost zero and ΔS° is positive, suggesting that the main interaction force is an electrostatic force [41].

The values of ΔS° , ΔH° and ΔG° for flavonoids binding to HAase are listed in Table 2. The negative value of ΔG° revealed that binding interactions between the flavonoids and HAase were spontaneous processes. The electrostatic interactions are the main driving force in the binding of HAase with seven flavonoids, and hydrophobic interaction was playing a major role in quercetin binding to HAase. Meanwhile, the different amounts of hydroxyls exist in molecular structure of these flavonoids, therefore, the hydrogen bonding formation might also participate in the binding processes.

Energy Transfer Between HAase and Flavonoids

According to Förster's non-radioactive energy transfer theory [42], if an acceptor could absorb the emitted fluorescence from a donor, energy may transfer from the donor to the acceptor. The distances (r) between donor (HAase) and acceptor (flavonoids) can be determined. The efficiency of energy transfer (E) related to the distance:

$$E = 1 - F_0 / F = R_0^6 / (R_0^6 + r^6) \quad (5)$$

where R_0 is the critical distance between the donor and acceptor when their transfer efficiency is 50 %. It is given by the following equation:

$$R_0^6 = 8.8 \times 10^{-25} K^2 \cdot \Phi \cdot N^{-4} \cdot J \quad (6)$$

where K^2 is the spatial orientation factor of the dipole, N is the refractive index of medium, Φ is the quantum yield of the donor, and J is the overlap integral of the fluorescence emission spectrum of the donor with the absorption spectrum of the acceptor (shown in Fig. 5), which can be calculated by the equation:

$$J = \sum \left[F(\lambda) \cdot \varepsilon(\lambda) \cdot \lambda^4 \cdot \Delta\lambda \left(\int \sum F(\lambda) \cdot \Delta\lambda \right) \right] \quad (7)$$

where $F(\lambda)$ is the fluorescence intensity of the fluorescence donor at wavelength λ , and $\varepsilon(\lambda)$ is the molar absorption coefficient of the acceptor at wavelength λ . In the present case, $K^2=2/3$, $N=1.366$, and $\Phi=0.118$ [43]. According to Eqs. (5–

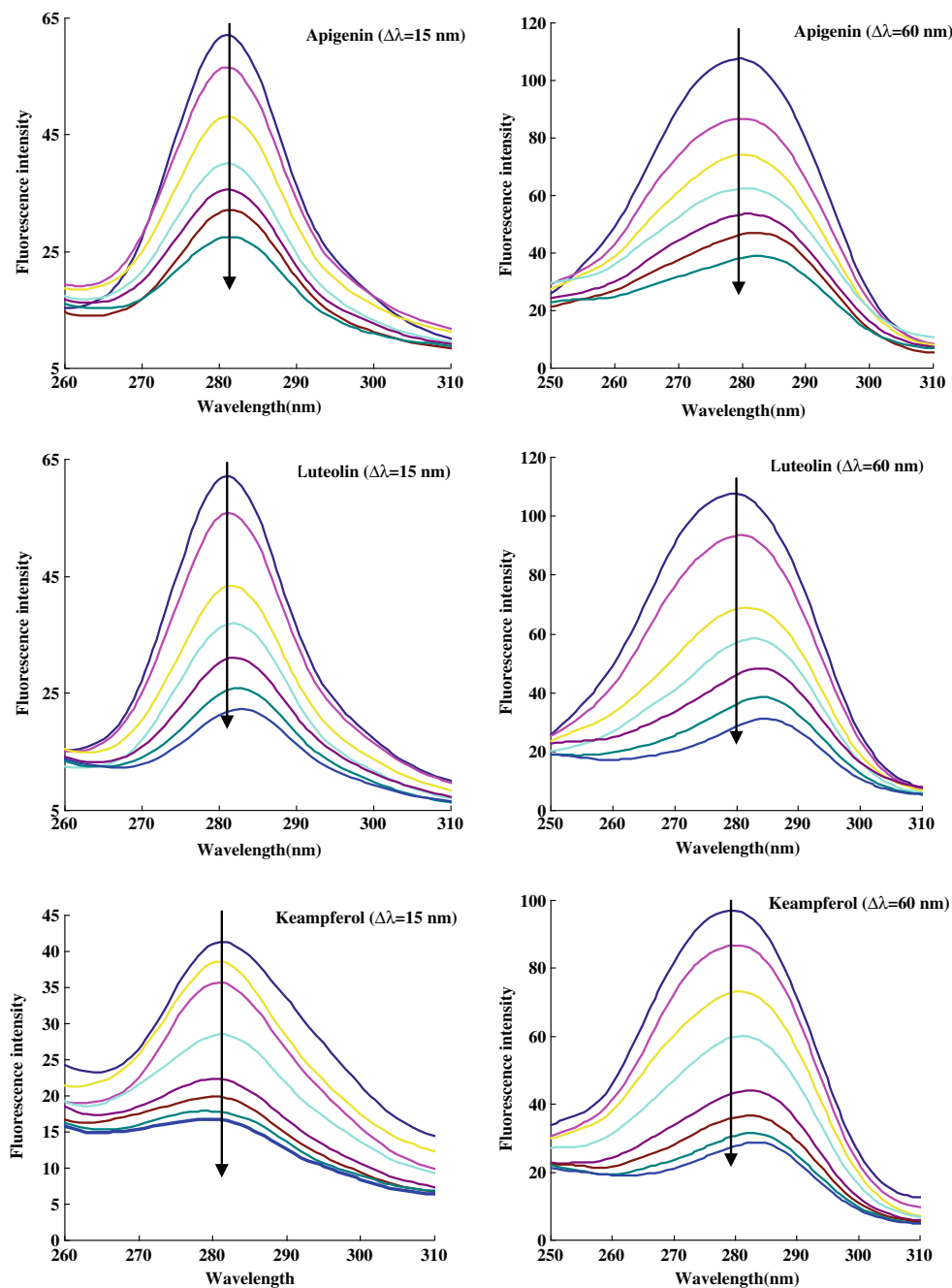


Fig. 6 Synchronous fluorescence spectra of interaction between HAase and flavonoids at room temperature. Conditions as same as Fig. 2

7), E , r , R_0 , and J of the flavonoid-HAase interaction could be calculated and listed in Table 3. the values of R_0 and r for flavonoids were all less than 7 nm, which indicated that the energy transfer from HAase to all flavonoids occurred with high probability. In accordance with prediction by Förster's non-radioactive energy transfer theory, these results indicate again the presence of static quenching mechanism in the interaction between flavonoids and HAase.

Conformational Investigations

Synchronous fluorescence spectra were developed in 1971 and were obtained by simultaneously scanning excitation and emission monochromators while maintaining a constant wavelength interval between them [44]. When the D-value ($\Delta\lambda$) between excitation and emission wavelength were set at 15 or 60 nm, the synchronous fluorescence

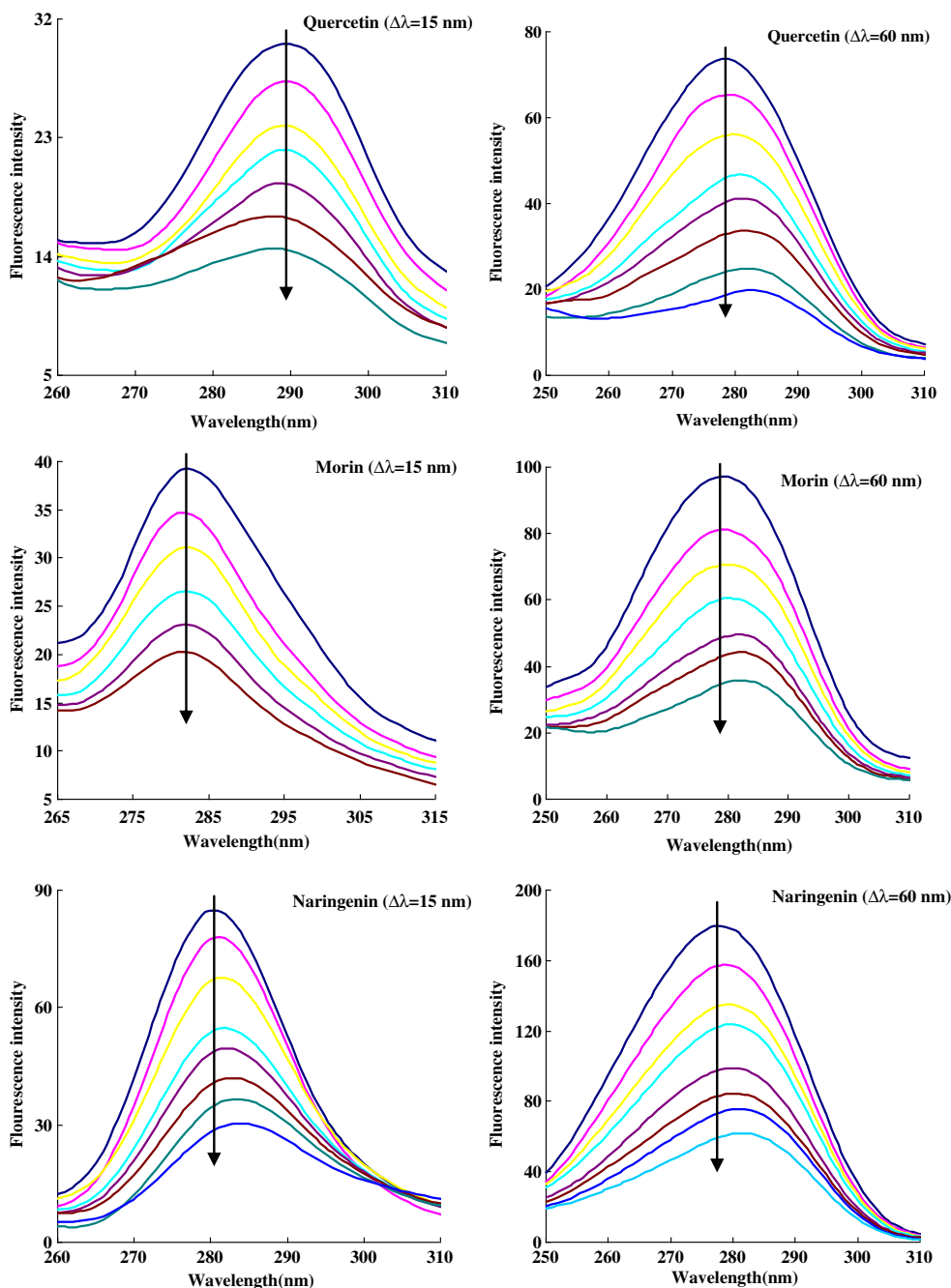


Fig. 6 (continued)

gives the characteristic information of tyrosine (Tyr) or tryptophan (Trp) residues in HAase, respectively [45]. By investigating the synchronous fluorescence spectra of Tyr and Trp residues, the conformational changes of HAase could be explored.

The synchronous fluorescence spectra of HAase upon addition of flavonoids at $\Delta\lambda=15$ and 60 nm were shown in Fig. 6. As the concentration of flavonoid increased

gradually, the synchronous fluorescence intensity decreased and a slight blue shift of Trp residues was observed in daidzein-HAase system, and an obvious red shift appeared in luteolin-HAase and naringenin-HAase systems. Moreover, the maximum emission wavelength of Trp residues had a significant red shift in all flavonoid-HAase systems. The red shift of the Tyr peak and Trp peak indicates that the conformation of HAase

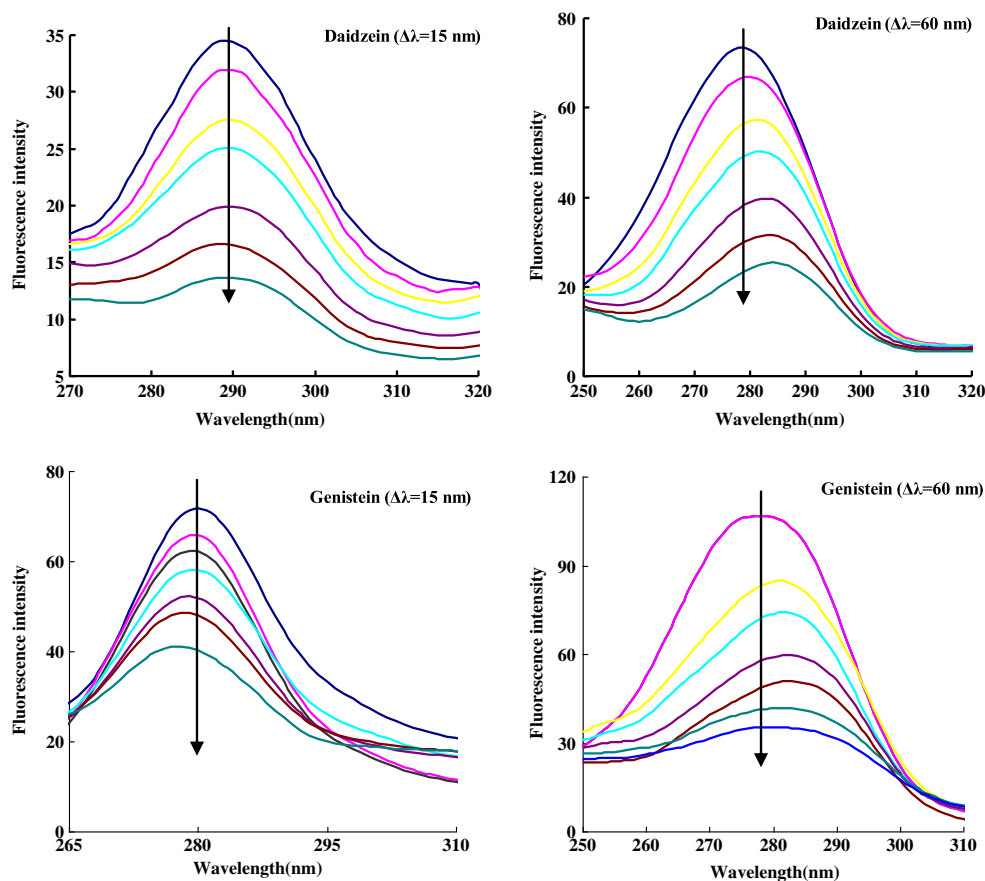


Fig. 6 (continued)

was changed and the polarity around the Tyr and Trp residues was increased and the hydrophobicity was decreased. In contrast, the blue shift of Tyr peak and Trp peak revealed that the hydrophobicity of the Tyr and Trp residues increased and both of them buried in the non-polar hydrophobic cavities were moved to a more hydrophobic environment.

Three-dimensional fluorescence spectroscopy is another powerful method for providing conformational and structural information of protein [46]. The three-dimensional fluorescence spectra of HAase and flavonoid-HAase systems were shown in Fig. 7. Peak 1 is the Rayleigh scattering peak ($\lambda_{em} = \lambda_{ex}$), Peak 2 ($\lambda_{ex}/\lambda_{em} = 278/330$ nm) mainly reveals the spectral feature of Tyr and Trp residues. Because when HAase is excited at 278 nm, it primarily displays the intrinsic fluorescence of Tyr and Trp residues, and the phenylalanine residue fluorescence can be negligible. In the absence of flavonoid, the relative fluorescence intensity of peak 2 and the stoke shift ($\lambda_{em} - \lambda_{ex}$) of HAase were 82.0 and 52 nm, respectively. However, after the addition of flavonoid, the relative

fluorescence intensity of Peak 2 and the stoke shifts had changed obviously, which indicated that the interactions between flavonoids and HAase induced microenvironment and conformation changed in HAase. Red shift of Peak 2 of HAase in the presence of flavonoid (from 330 to 335 nm) suggested that the Trp residues were brought to a more hydrophilic environment. These results were consistent with those of fluorescence quenching and synchronous fluorescence spectra.

Modeling Study of the Bindings Between Flavonoid and HAase

In order to study the binding between flavonoid and HAase systematically, to identify the precise binding sites and the exact conformation of flavonoid at the binding sites, a docking program was run to simulate the binding mode between flavonoid and HAase. From the docking calculation, the lowest energy-ranked results of flavonoid-HAase conformations

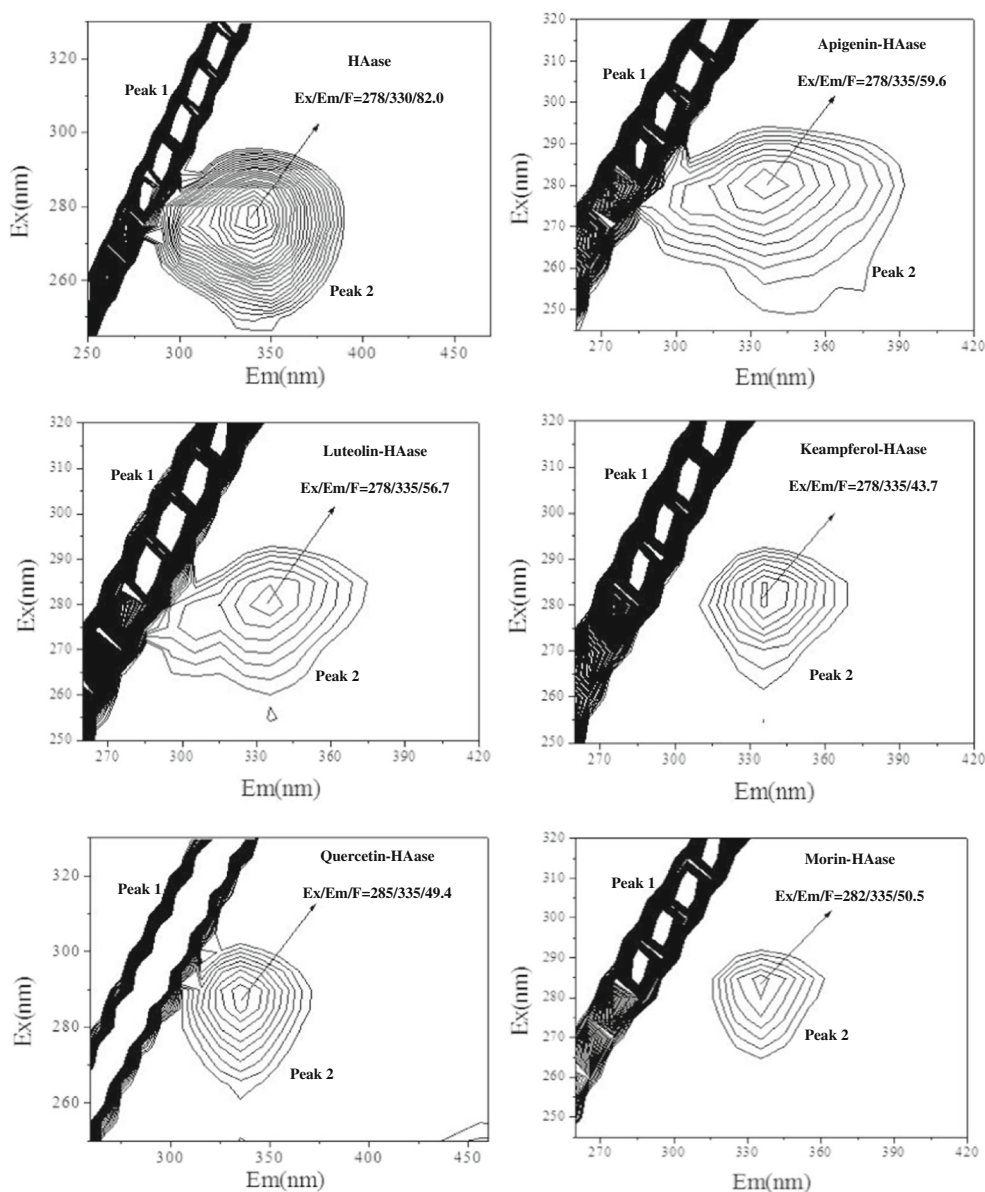


Fig. 7 The three-dimensional fluorescence contour spectra of HAase and flavonoid-HAase systems. Conditions: $C_{\text{Apigenin}}=12 \times 10^{-6} \text{ mol} \cdot \text{L}^{-1}$, $C_{\text{Luteolin}}=24 \times 10^{-6} \text{ mol} \cdot \text{L}^{-1}$, $C_{\text{Keampferol}}=16 \times 10^{-6} \text{ mol} \cdot \text{L}^{-1}$, $C_{\text{Quercetin}}=$

$16 \times 10^{-6} \text{ mol} \cdot \text{L}^{-1}$, $C_{\text{Morin}}=24 \times 10^{-6} \text{ mol} \cdot \text{L}^{-1}$, $C_{\text{Naringenin}}=42 \times 10^{-6} \text{ mol} \cdot \text{L}^{-1}$, $C_{\text{Daidzein}}=30 \times 10^{-6} \text{ mol} \cdot \text{L}^{-1}$, $C_{\text{Genistein}}=22 \times 10^{-6} \text{ mol} \cdot \text{L}^{-1}$; $C_{\text{HAase}}=0.1 \times 10^{-5} \text{ mol} \cdot \text{L}^{-1}$

were summarized in Table 4. By comparison of the data from Table 2 with the data from Table 4, it can be seen that the observed free energy change of binding (ΔG°) for flavonoid-HAase systems was not extremely close to the experimental data. The reasons for this result may be the differences between the X-ray structure of the HAase in crystal and that of the aqueous system in this study.

As usual, the total binding free energy can be divided into electrostatic energy and nonelectrostatic energy, such as hydrophobic, polar and hydrogen bond. As shown in Fig. 8, all flavonoids were located in the hydrophobic cavity of HAase

and were surrounded by the hydrophobic and hydrophilic amino acids (shown in Table 5). Therefore, it can be concluded that the interaction between flavonoid and HAase is mainly electrostatic forces and hydrophobic interactions in nature. However, due to more hydrophobic amino acids lining quercetin in the binding site, hydrophobic interaction was more prominent than electrostatic force in quercetin-HAase system. These results were consistent with the results obtained from the thermodynamic parameter analysis. As shown in Table 5, several amino acid residues, such as Tyr75, Asp129, Glu131, Tyr202, Tyr247, Tyr286, Gln288, Asp292 and Trp321, ap-

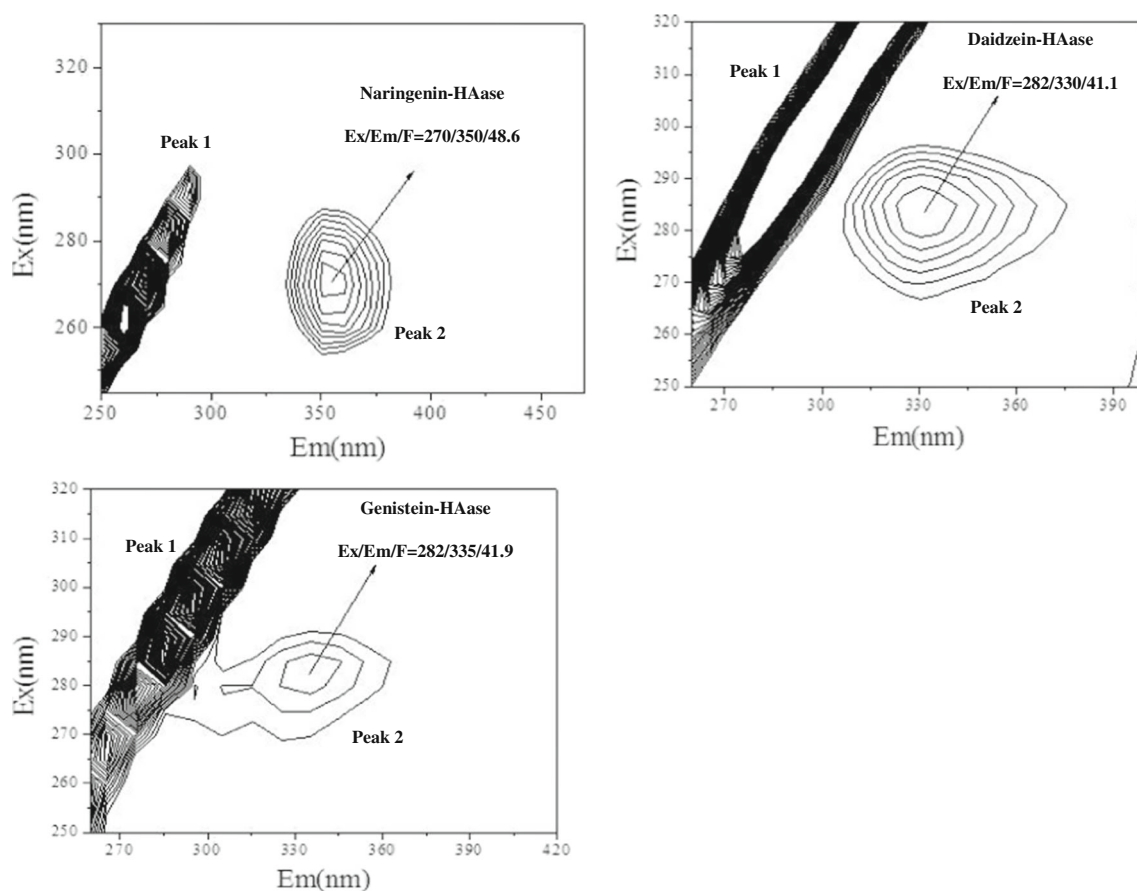


Fig. 7 (continued)

peared in the binding of each flavonoid with HAase. These results indicated that these residues would play a very important role in the interaction between flavonoid and HAase and might constitute the catalytic site of HAase. Moreover, due to the presence of several ionic and polar groups, there are also considerable numbers of hydrogen bonds in flavonoid-HAase systems. As shown in Table 5, one of the hydrogen bonds is formed with the Asp129 and/or Asp292 residues in all flavonoid-HAase systems. It can be assumed from these

results that the catalytic site of HAase, like pepsin [47] and rennin [48], was formed by two Asp residues, Asp129 and Asp292, one of which has to be protonated, and the other deprotonated, for the protein to be active. Therefore, according to docking and fluorescence results, it could be speculated that flavonoid bound directly into the enzyme cavity site and the binding of flavonoid into the enzyme cavity influenced the microenvironment of the catalytic site, which would inhibit the activity of HAase.

Table 4 The lowest energy-ranked results of flavonoid-HAase binding conformations

Flavonoid	Binding energy (kcal mol ⁻¹)	Ligand efficiency	Internal energy
Apigenin	-5.9 (-24.70 kJ mol ⁻¹)	-0.3	-6.73
Luteolin	-5.98 (-25.03 kJ mol ⁻¹)	-0.28	-7.02
Keampferol	-6.15 (-25.74 kJ mol ⁻¹)	-0.29	-7.14
Quercetin	-6.46 (-27.04 kJ mol ⁻¹)	-0.29	-7.41
Morin	-5.74 (-24.03 kJ mol ⁻¹)	-0.26	-6.61
Naringenin	-5.8 (-24.28 kJ mol ⁻¹)	-0.29	-7.06
Daidzein	-6.47 (-27.08 kJ mol ⁻¹)	-0.34	-7.02
Genistein	-6.66 (-27.88 kJ mol ⁻¹)	-0.33	-7.18

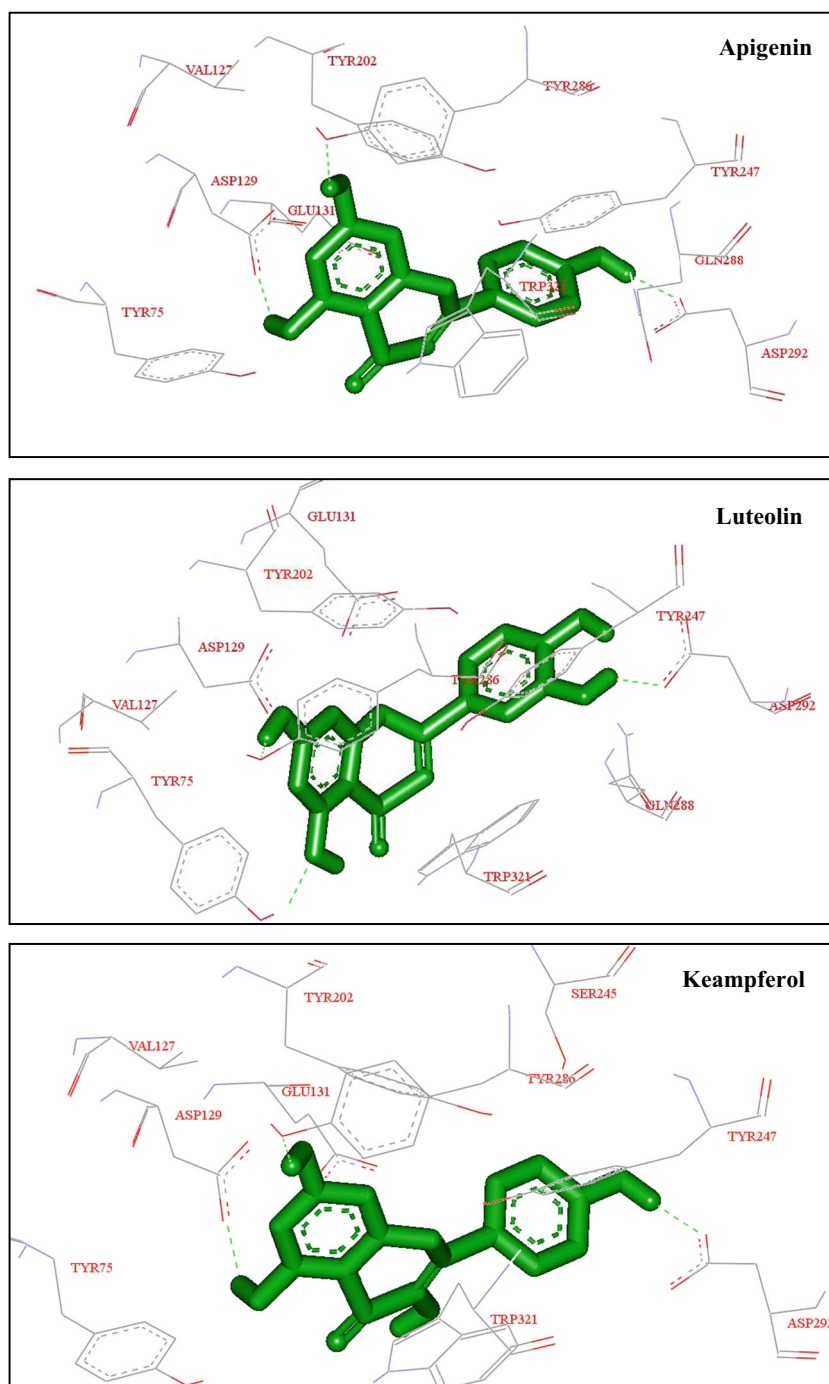


Fig. 8 Docked pose corresponding to the minimum energy conformation for flavonoid binding to HAase cavity. Detailed illustration of the amino acid residues lining the binding site in the HAase cavity. Green molecule displays flavonoids; broken lines display hydrogen bonds

Conclusion

In this study, the interactions between HAase and flavonoids exhibiting wide range of physiological activities especially in anti-inflammatory and anti-allergic were

investigated by a combination of experimental and computational methods. Each flavonoid can quench the fluorescence of HAase via static quenching. Based on the results of binding capacity, calculated thermodynamic parameters and molecular modeling study, it was

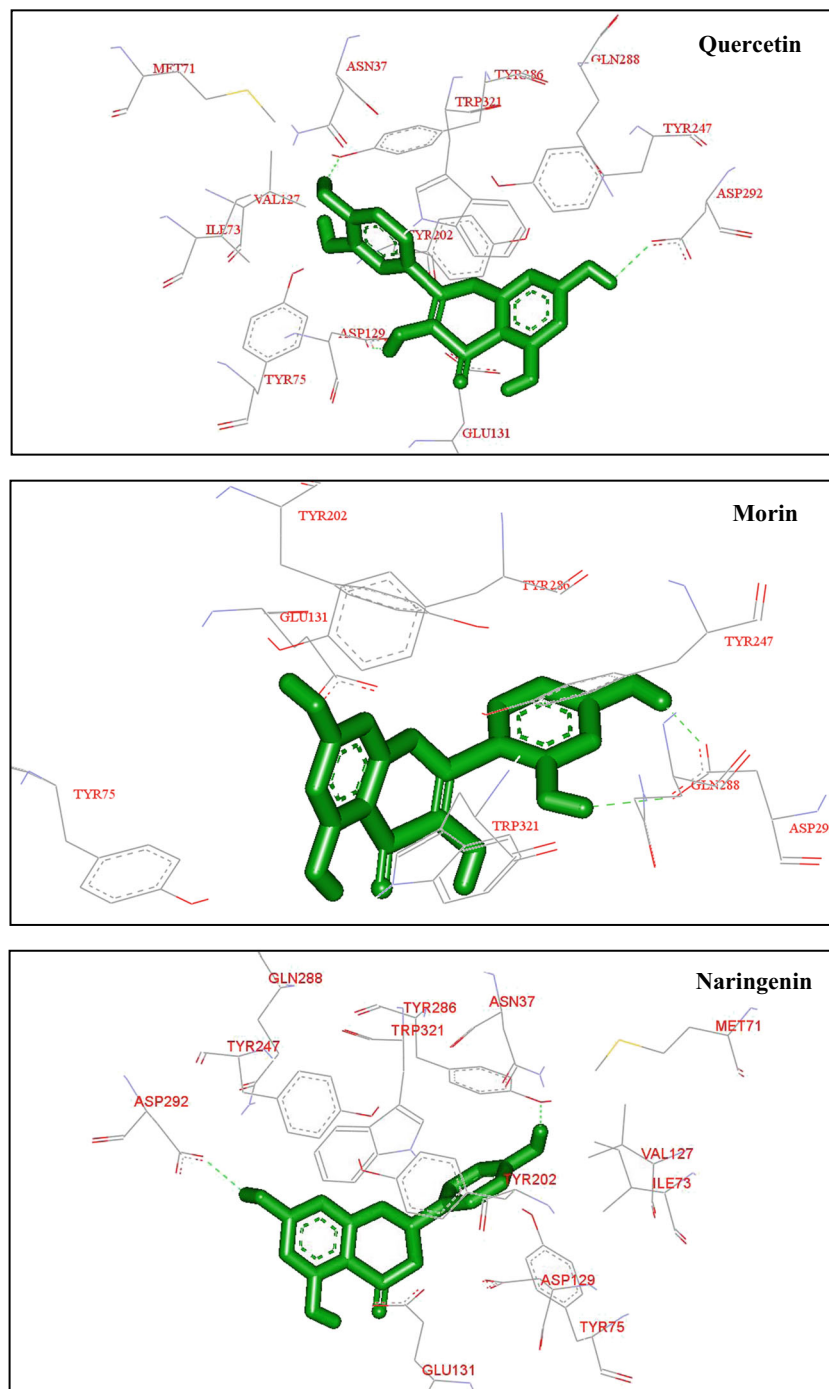


Fig. 8 (continued)

concluded that each flavonoid could spontaneously bind with HAase mainly through electrostatic forces, as well as hydrophobic interactions and hydrogen bonding. The synchronous and three-dimensional fluorescence spectra revealed that microenvironment and conformation of HAase were demonstrably changed in the presence of flavonoid. Since the binding of flavonoid affected the

microenvironment of the HAase activity site, flavonoid caused the inhibition of HAase activity. All these experimental results and theoretical data in this study would be helpful in understanding the mechanism of inhibitory effects of flavonoid against HAase and explaining the anti-inflammatory mechanism of some TCMs as anti-inflammatory drugs.

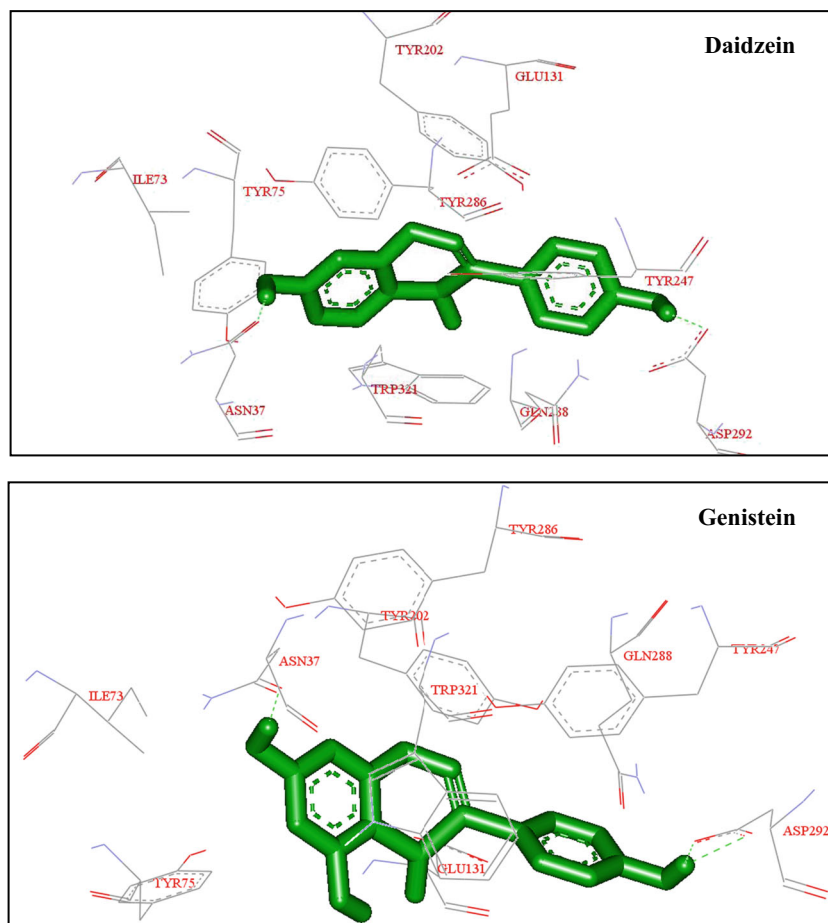


Fig. 8 (continued)

Table 5 The amino acid residues lining the binding site in HAase cavity and hydrogen bonds between flavonoid and HAase

Flavonoids	Amino acid residues lining the binding site and hydrogen bonds		
	Hydrophobic amino acid	Hydrophilic amino acid	Hydrogen bond
Apigenin	Tyr75*, Val127, Tyr202*, Tyr247*, Tyr286*, Trp321*	Asp129*, Glu131*, Gln288*, Asp292*	Asp129 (1.8624 Å), Tyr286 (2.3539 Å), Asp292 (1.9174 Å)**
Luteolin	Tyr75*, Val127, Tyr202*, Tyr247*, Tyr286*, Trp321*	Asp129*, Glu131*, Gln288*, Asp292*	Tyr75 (1.9603 Å), Tyr286 (1.9700 Å), Asp292 (1.8364 Å)**
Keampferol	Tyr75*, Val127, Tyr202*, Tyr247*, Tyr286*, Trp321*	Asp129*, Glu131*, Gln288*, Asp292*	Asp129 (1.9654 Å), Tyr286 (2.2922 Å), Asp292 (1.8954 Å)**
Quercetin	Met71, Ile73, Tyr75*, Val127, Tyr202*, Tyr247*, Tyr286*, Trp321*	Asn37, Asp129*, Glu131*, Gln288*, Asp292*	Asp129 (1.6714 Å), Tyr286 (1.6805 Å), Asp292 (2.2390 Å)**
Morin	Tyr75*, Tyr202*, Tyr247*, Tyr286*, Trp321*	Glu131*, Gln288*, Asp292*	Asp292 (1.8984 Å)***, Asp292 (2.4276 Å)**
Naringenin	Met71, Ile73, Tyr75*, Val127, Tyr202*, Tyr247*, Tyr286*, Trp321*	Asn37, Asp129*, Glu131*, Gln288*, Asp292*	Tyr286 (1.7105 Å), Asp292 (2.1644 Å)**
Daidzein	Ile73, Tyr75*, Tyr202*, Tyr247*, Tyr286*, Trp321*	Asn37, Glu131*, Gln288*, Asp292*	Asn37 (1.8764 Å), Asp292 (2.1536 Å)**
Genistein	Ile73, Tyr75*, Tyr202*, Tyr247*, Tyr286*, Trp321*	Asn37, Glu131*, Gln288*, Asp292*	Asn37 (1.7493 Å), Asp292 (2.3171 Å)***, Asp292 (2.1005 Å)**

* The common amino acid residues lining the flavonoids in the binding site

** The common amino acid residue forming the hydrogen bond with flavonoids

Acknowledgments We grateful acknowledge the financial support of the National Natural Science Foundation of China (U1304823).

References

- Gautam R, Jachak SM (2009) Recent developments in anti-inflammatory natural products. *Med Res Rev* 29:767–820
- Yahaya YA, Don MM, Yahaya AS (2014) The effect of culture conditions on the growth of *T. lactinea* and anti-inflammatory activities via in vitro inhibition of hyaluronidase and lipoxygenase enzyme activities. *J Taiwan Inst Chem Eng* 45:2054–2059
- Duthie ES, Chain EA (1939) A mucolytic enzyme in tests extract. *Nature* 144:977–978
- Kakegawa H, Matsumoto H, Satoh T (1999) Inhibitory effects of some natural products on the activation of hyaluronidase and their anti-allergic action. *Chem Pharm Bull* 40:1439–1442
- Cameron E, Pauling L, Leibovitz B (1979) Ascorbic acid and cancer: a review. *Cancer Res* 39:663–681
- Meyer K (1947) The biological significance of hyaluronic acid hyaluronidase. *Physiol Rev* 27:335–359
- Lee KK, Choi JD (1999) The effects of *Areca catechu* L. extract on anti-inflammation and anti-melanogenesis. *Int J Cosmet Sci* 21:275–284
- Shibata T, Fujimoto K, Nagayama K, Yamaguchi K, Yamaguchi K, Nakamura T (2002) Inhibitory activity of brown algal phlorotannins against hyaluronidase. *Int J Food Sci Technol* 37:703–709
- Furusawa M, Narita Y, Iwai K, Fukunaga T, Nakagiri O (2011) Inhibitory effect of a hot water extract of coffee ‘silverskin’ on hyaluronidase. *Biosci Biotechnol Biochem* 75:1205–1207
- Liu M, Yin H, Dong JJ, Xiao L, Liu G, Qian ZH, Miao JL (2013) Inhibition and interaction with hyaluronidase by compounds from Hop (*Humulus lupulus* L.) flowers. *Asian J Chem* 25:10262–10266
- Heim KE, Tagliaferro AR, Bobilya DJ (2002) Flavonoid antioxidants: chemistry, metabolism and structure-activity relationships. *J Nutr Biochem* 13:572–584
- Graf BA, Milbury PE, Blumberg JB (2005) Flavonols, flavones, flavanones, and human health: epidemiological evidence. *J Med Food* 8:281–290
- Wang YC, Huang KM (2013) In vitro anti-inflammatory effect of apigenin in the helicobacter pylori-infected gastric adenocarcinoma cells. *Food Chem Toxicol* 53:376–383
- Zhang XX, Wang GJ, Gurley EC, Zhou HP (2014) Flavonoid apigenin inhibits lipopolysaccharide-induced inflammatory response through multiple mechanisms in macrophages. *PLoS One* 9:e107072
- Megumi FT, Kei N, Kenji T, Tadahiko M, Tadashi K (2011) Anti-inflammatory activity of structurally related flavonoids, apigenin, luteolin and fisetin. *Int Immunopharmacol* 11:1150–1159
- Jeon IH, Kim HS, Kang HJ, Lee HS, Jeong SI, Kim SJ, Jang SI (2014) Anti-inflammatory and antipruritic effects of luteolin from *Perilla* (*P. frutescens* L.) leaves. *Molecules* 19:6941–6951
- Peramaiyan R, Thamaraiselvan R, Natarajan N, Rajendran P, Yutaka N, Ikuo N (2014) Kaempferol, a potential cytostatic and cure for inflammatory disorders. *Eur J Med Chem* 86:103–112
- Yilmaz MZ, Guzel A, Torun AC, Okuyucu A, Salis O, Karli R, Gacar A, Guvenc T, Paksu S, Urey V, Murat N, Alacam H (2014) The therapeutic effects of anti-oxidant and anti-inflammatory drug quercetin on aspiration-induced lung injury in rats. *J Mol Histol* 45:195–203
- Galvez J, Coelho G, Crespo ME, Cruz T, Rodriguez-Cabezas ME, Concha A, Gonzalez M, Zarzuelo A (2001) Intestinal anti-inflammatory activity of morin on chronic experimental colitis in the rat. *Aliment. Pharm Ther* 15:2027–2039
- Jung HJ, Kim SJ, Song YS, Park EH, Lim CJ (2010) Evaluation of the antiangiogenic, anti-inflammatory, and antinociceptive activities of morin. *Planta Med* 76:273–275
- Jayaraman J, Jesudoss VAS, Menon VP, Namasivayam N (2012) Anti-inflammatory role of naringenin in rats with ethanol induced liver injury. *Toxicol Mech Methods* 22:568–576
- Tsai SJ, Huang CS, Mong MC, Kam WY, Huang HY, Yin MC (2012) Anti-inflammatory and antifibrotic effects of naringenin in diabetic mice. *J Agric Food Chem* 60:514–521
- Liu MH, Lin YS, Sheu SY, Sun JS (2009) Anti-inflammatory effects of daidzein on primary astroglial cell culture. *Nutr Neurosci* 12:123–134
- Verdrengh M, Jonsson IM, Holmdahl R, Tarkowski A (2003) Genistein as an anti-inflammatory agent. *Inflamm Res* 52:341–346
- Ji GY, Yang QH, Hao J, Guo LN, Chen X, Hu JP, Leng L, Jiang ZQ (2011) Anti-inflammatory effect of genistein on non-alcoholic steatohepatitis rats induced by high fat diet and its potential mechanisms. *Int Immunopharmacol* 11:762–768
- Kuppusamy UR, Das NP (1991) Inhibitory effects of flavonoids on several venom hyaluronidases. *Experientia* 47:1196–1200
- Moon SH, Kim KT, Lee NK (2009) Inhibitory effects of naringenin and its novel derivatives on hyaluronidase. *Food Sci Biotechnol* 18:267–270
- Lee JH, Kim GH (2010) Evaluation of antioxidant and inhibitory activities for different subclasses flavonoids on enzymes for *Rheumatoid arthritis*. *J Food Sci* 75:H212–H217
- China Pharmacopoeia Committee (2010) Pharmacopoeia of the People’s Republic of China. Chemical Industry Press, Beijing
- Frokjaer S, Otzen DE (2005) Protein drug stability: a formulation challenge. *Nat Rev Drug Discov* 4:298–306
- Cheatum CM (2013) Drug-protein interactions: mechanisms of potency. *Nat Chem* 5:152–153
- Madrakian T, Bagheri H, Afkhami A, Soleimani M (2014) Spectroscopic and molecular docking techniques study of the interaction between oxymetholone and human serum albumin. *J Lumin* 155:218–225
- Zeng HJ, Qi TT, Yang R, You J, Qu LB (2014) Spectroscopy and molecular docking study on the interaction behavior between nobiletin and pepsin. *J Fluoresc* 24:1031–1040
- Yang R, Yu LL, Zeng HJ, Liang RL, Chen XL, Qu LB (2012) The interaction of flavonoid-lysozyme and the relationship between molecular structure of flavonoids and their binding activity to lysozyme. *J Fluoresc* 22:1449–1459
- Lakowicz JR, Weber G (1973) Quenching of protein fluorescence by oxygen. Detection of structural fluctuations in proteins on the nanosecond time scale. *Biochemistry* 12:4171–4179
- Zhang YZ, Zhou B, Zhang XP, Huang P, Li CH, Liu Y (2009) Interaction of malachite green with bovine serum albumin: determination of the binding mechanism and binding site by spectroscopic methods. *J Hazard Mater* 163:1345–1352
- Chi ZX, Liu RT, Zhang H (2010) Noncovalent interaction of oxytetracycline with the enzyme trypsin. *Biomacromolecules* 11:2454–2459
- Bi SY, Ding L, Tian Y, Song DQ, Zhou X, Liu X, Zhang HQ (2004) Investigation of the interaction between flavonoids and human serum albumin. *J Mol Struct* 703:37–45
- Pessini AC, Takao TT, Cavalheiro EC, Vichnewski W, Sampaio SV, Giglio JR, Arantes EC (2001) A hyaluronidase from *Tityus serrulatus* scorpion venom: isolation, characterization and inhibition by flavonoids. *Toxicon* 39:1495–1504
- Li S, Huang KL, Zhong M, Guo J, Wang WZ, Zhu RH (2010) Comparative studies on the interaction of caffeic acid, chlorogenic acid and ferulic acid with bovine serum albumin. *Spectrochim Acta A* 77:680–686

41. Ross PD, Subramanian S (1981) Thermodynamics of protein association reactions: forces contributing to stability. *Biochemistry* 20: 3096–3102
42. Förster T (1948) Zwischenmolekulare energiewanderung und fluoreszenz. *Ann Phys* 437:55–75
43. Jin J, Zhang X (2008) Spectrophotometric studies on the interaction between pazufloxacin mesilate and human serum albumin or lysozyme. *J Lumin* 128:81–86
44. Wang YQ, Zhang HM, Zhang GC, Liu SX, Zhou QH, Fei ZH, Liu ZT (2007) Studies of the interaction between parquat and bovine hemoglobin. *Int J Biol Macromol* 41:243–250
45. Guo M, Lu WJ, Li MH, Wang W (2008) Study on the binding interaction between carnitine optical isomer and bovine serum albumin. *Eur J Med Chem* 43:2140–2148
46. Dong CY, Ma SY, Liu Y (2013) Studies of the interaction between demeclocycline and human serum albumin by multi-spectroscopic and molecular docking methods. *Spectrochim Acta A* 103:179–186
47. Antonov VK, Ginodman LM, Kapitannikov YV, Barshevskaya TN, Gurova AG, Rumsh LD (1978) Mechanism of pepsin catalysis: general base catalysis by the active-site carboxylate ion. *FEBS Lett* 88:87–90
48. Danser AH, Deinum J (2005) Renin, prorenin and the putative (pro) renin receptor. *Hypertension* 46:1069–1076